Journal of Solid Mechanics Vol. 13, No. 2 (2021) pp. 213-232
DOI: 10.22034/jsm.2020.1901736.1607

Analysis of Nanoplate with a Central Crack Under Distributed Transverse Load Based on Modified Nonlocal Elasticity Theory

M. Rajabi [1], H. Lexian [2,*], A. Rajabi [1]

[1] *Mechanical Engineering, Malek Ashtar University of Technology (MUT), Tehran, Iran*
[2] *Faculty of Material & Manufacturing Technology, Malek Ashtar University of Technology (MUT),Tehran, Iran*

Received 6 March 2021; accepted 4 May 2021

ABSTRACT

In this paper, using the complete modified nonlocal elasticity theory, the deflection and strain energy equations of rectangular nanoplates, with a central crack, under distributed transverse load were overwritten. First, the deflection of nanoplate was obtained using Levy's solution and consuming it; strain energy of nanoplate was found. As regards nonlocal elasticity theory wasn't qualified for predicting the static behavior of nanoplates under distributed transverse load, using modified nonlocal elasticity theory, the deflection of nanoplate with a central crack for different values of the small-scale effect parameter was achieved. It was gained with the convergence condition for the complete modified nonlocal elasticity theory. To verify the result, the results for the state of the small-scale effect parameter were placed equal to zero (plate with macro-scale) and then were compared with the numerical results as well as the classical analytical solution results available in the valid references. It was shown that the complete modified nonlocal elasticity theory does not show any singularity at the crack-tip unlike the classical theory; therefore, the method presented is a suitable method for analysis of the nanoplates with a central crack.

Keywords: Nonlocal elasticity theory; Crack; Small-scale effect; Nanoplate; Singularity.

1 INTRODUCTION

DISTINCT methods are depending on the materials' scale for investigation and analyzing their behavior under different loading and boundary conditions, each of which has its application according to the problem definition, and the required accuracy in the results. The limitations of experimental methods and quantum mechanics (although it is very precise) have led to the interest of molecular methods. However, molecular models were unsuitable for the analysis of large structures, and consequently; continuum mechanics were considered. Defects of crystal lattice such as atoms' vacancy, dislocation, the existence of very small cracks, etc. can cause many

*Corresponding author. Tel.: +98 22987686; Fax: +98 22936578.
E-mail address: Lexian@mut.ac.ir (H.Lexian).

problems, including reduction of material strength. Many of these flaws can be simulated as very small cracks. Models of the classical continuum mechanics are scale-free and can't account for quantum effects, whereas the analysis of such defects must be performed on a nano-scale [1]. Therefore, several modified theories such as Eringen's nonlinear elasticity theory, strain gradient theory, couple-stress theory, and modified couple-stress theory have been proposed, which are capable of considering the small-scale effect. Among these theories, the theory of nonlocal elasticity has been more widely accepted because of its simplicity and proper prediction of nanomaterial behavior and also its concordance with molecular dynamics results. As regards it has not complex calculations, this theory is capable of analyzing large-scale structures and as the following is discussed, it is a very good method for investigating and identifying crack parameters in structures. In 1999, Gao [2] presented a general theory of nonlocal elasticity, which was very effective in rediscovering Eringen's nonlocal elasticity theory. Assuming the symmetry of the parameters of the nonlocal elasticity theory, Gao developed the theory based on the micron-scale behavior of the crystalline lattice and by reducing the relationships in the nonlocal elasticity theory, he proposed a higher-order gradient model called the couple-stress theory. The nonlocal elasticity theory enabled the researchers to solve many of the problems encountered with stress singularity in the local elasticity (such as crack-tip problems) and to show that this singularity disappears with nonlocal behavior. Many researchers have considered the analysis of cracked nanoplates under in-plane load and also have paid attention the singularity at the crack-tip such as Zhou et. al that obtained stress in a plate containing a crack, which was under out-of-plane shear stress, with using the nonlocal elasticity equations. The results [3] were shown that there is not any singularity of stress at the crack-tip. In 2003, Zhou et. al [4] used these results to predict crack behavior in piezoelectric materials. They obtained a stress field at the crack-tip that depends on the crack length and the internal length of the material lattice. Zhou and Shen [5] studied the propagation of harmonic shear stress waves by the same-direction cracks on a plane using the nonlocal elasticity theory and obtained the stress field at the crack-tip, which depends on the crack length, and also were observed that there isn't any singularity at it. In 2003, Zhou and Wang [6] used the results for piezoelectric materials and validated these results. In 2005, Zhou and Wang [8] investigated the interaction of two parallel cracks in the functionally graded materials under out-of-plane shear loading by nonlocal elasticity theory using the Schmidt method, which their results showed there isn't any stress singularity near the crack-tip. They showed that the stress field at the crack-tip, in addition to the crack length and lattice parameter, depends on the distance between the two cracks from each other, and the characteristic parameter of the functionally graded materials (FGM). Subsequently, the bending of non-cracked nanoplates has attracted the attention of many researchers through various theories. In 2012, Huang et. al [9] calculated the small-scale effect parameter for single-layer graphene sheets. They considered single-layer graphene sheets as rectangular sheets with simply-supported at all four edges under transverse concentrated load in the middle of the plate and obtained their deflection using both nonlocal elasticity and molecular dynamics. They concluded that the nonlocal parameter is not constant and depends on the sheet dimensions, and this dependence is different for the Zigzag and armchair graphene sheets. In 2015, Yan et. al [10] used the nonlocal elasticity method to obtain higher-order unlimited differential equations for non-cracked nanoplate and nanobeam models. They investigated the small-scale effect parameter on nanobeam and nanoplate deflection and obtained very close results to molecular dynamics simulations. In 2015, Rezatalab and Golmakani [11] investigated the nonlinear bending of graphene rectangular nanoplates in a two-parameter polymeric environment under uniform transverse load by the Eringen's nonlocal model. They obtained equilibrium equations based on the Mindlin's rectangular plates using Von-Karman's strains and also, applied the Eringen's nonlocal theory to consider the small-scale effect. They showed that by increasing the small-scale effect parameter, the deflection of nanoplate decreases. In 2016, Şeref [12] analyzed the static analysis of rectangular nanoplates under distributed transverse load based on the couple-stress theory using differential quadrature method. He showed that the geometrical properties, and the small-scale effect parameter play an important role in the show the bending behavior of nanoplates under distributed transverse load. In 2017, Eskandari et. al [13] analyzed bending of the Kirchhoff's graphene rectangular nanoplate using modified couple-stress theory and simply-supported boundary conditions. Gaining strain energy and external force and placing them in Hamilton's principle, they obtained the basic and auxiliary equations of the nanoplate and used the Navier method to analyze the nanoplate. In 2018, Sadatmosavi et. al [14] showed that the nonlocal elasticity theory in some static problems, such as nanobeam and nanoplate bending with the simply-supported under concentrated and distributed transverse load, is not able to account for the small-scale effect parameter. Creating changes in nonlocal structural equations and introducing the complete modified nonlocal elasticity model, they obtained maximum deflection of nanobeam and nanoplate with simply-supported boundary conditions and also under concentrated and distributed transverse load. Furthermore, they extended efficiency of nonlocal elasticity theory in the field. Researcher have been frequently focused on analysis of the cracked plates under transverse load over the last few decades. For example, Shvabyuk et. al [15], studied bending of orthotropic plates containing a central crack. Their analytical model modified and improved bending theory of plates and also, it

explains transverse deformation of plate. Chattopadhyay [16] also presented an analytical solution to obtain the bending stress intensity factor using the Reissner's plate theory and Fourier integral method. He obtained the general formula of bending moment and twisting moment of infinite elastic plates, which contain cracks located on a single line.However, the present analysis suggests that the analysis of cracked nanoplates under transverse load has not yet been considered and also is one of the fields that need for more research. The nonlocal elasticity theory has wide application in the analysis of the nanoplates as well as fracture mechanics, which can be extended to the analysis of cracked nanoplates under transverse load.

In the present study, a complete modified nonlocal elasticity theory for static bending analysis of nanoplate with a central crack in two modes: 1. simply-support at all four edges and 2. Simply-supported at two edges and clamped-supported at the other two edges, are used. Furthermore, their deflection and strain energy equations have been obtained, and the lack of singularity existence at the crack-tip has been demonstrated.

2 RELATIONSHIPS GOVERNING STATIC BENDING OF CENTREAL CRACHED RECTANGULAR NANOPLATES

Using the complete modified nonlocal elasticity theory, it is possible to analyze the static bending of nanoplates under a concentrated and distributed transverse load. The cracked nanoplate is assumed and also, its thickness is t_p.

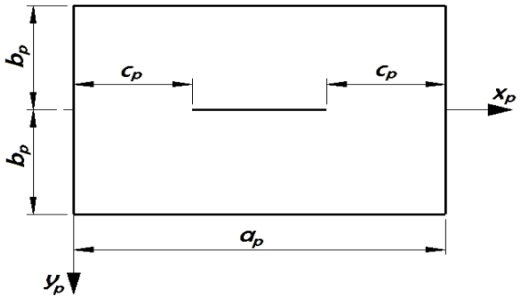

Fig.1
Rectangular nanoplate with a central crack.

According to classical theory, the displacement and strain fields are defined as follows:

$$U=\begin{Bmatrix}u_p(x,y)\\ v_p(x,y)\\ w_p(x,y)\end{Bmatrix}=\begin{Bmatrix}u_{p0}(x,y)-zw_{p,x}(x,y)\\ v_{p0}(x,y)-zw_{p,y}(x,y)\\ w_p(x,y)\end{Bmatrix},\varepsilon=\begin{Bmatrix}\varepsilon_x\\ \varepsilon_y\\ 2\varepsilon_{xy}\end{Bmatrix}=\begin{Bmatrix}u_{p0,x}-z_pw_{p,xx}\\ v_{p0,y}-z_pw_{p,yy}\\ u_{p0,y}+v_{p0,x}-2z_pw_{p,xy}\end{Bmatrix}=\varepsilon \tag{1}$$

$$z_pk,\qquad k=\begin{Bmatrix}k_x\\ k_y\\ 2k_{xy}\end{Bmatrix}=\begin{Bmatrix}W_{,x}\\ W_{,y}\\ 2W_{,xy}\end{Bmatrix}$$

where in U_p, V_p and W_p are the displacements in the three directions x_p, y_p and z_p respectively, and Also, U_{po} and V_{po} are in-plane displacement of the middle-plane. Assuming, E_p and v_p are the elastic module and Poisson's ratio of the nanoplate, respectively, according to the plane stress assumption, the local stress-strain relationship is defined as follows:

$$\boldsymbol{\sigma}^l=\begin{Bmatrix}\sigma_x^l\\ \sigma_y^l\\ \sigma_{xy}^l\end{Bmatrix}=\frac{E_p}{1-\nu_p^2}\begin{bmatrix}1 & \nu_p & 0\\ \nu_p & 1 & 0\\ 0 & 0 & (1-\nu_p)/2\end{bmatrix}\begin{Bmatrix}\varepsilon_x\\ \varepsilon_y\\ 2\varepsilon_{xy}\end{Bmatrix}=\mathbf{C}\boldsymbol{\varepsilon} \tag{2}$$

According to the nonlocal elasticity theory, the nonlocal constitutive equations can be expressed as follows [1]:

$$(1-N)\boldsymbol{\sigma}^{nl}=\boldsymbol{\sigma}^{l},\quad \boldsymbol{\sigma}^{nl}=\left\{\sigma_x^{nl}\quad \sigma_y^{nl}\quad \sigma_{xy}^{nl}\right\}^T \tag{3}$$

In which $\boldsymbol{\sigma}^{nl}$ and N are the nonlocal stress tensor and the nonlocal operator, respectively, and also are defined as follows:

$$N=\mu^2 L_e{}^2\nabla^2,\ \mu=\frac{e_0 L_i}{L_e} \tag{4}$$

where in μ is the dimensionless nonlocal parameter, L_i is the internal length (the distance between the carbon atoms), L_e is the external length, which is usually considered equal to the length of the nanoplate ([9] and [14]), and e_0 is the intrinsic properties of the material, which is obtained from experimental results or lattice dynamics atomic modeling. In the complete modified nonlocal elasticity theory, modified nonlocal equations are used instead of nonlocal structural Eqs. (3). The complete modified nonlocal constitutive equations can be described as follows:

$$\boldsymbol{\sigma}^{nl}=N^{*}\boldsymbol{\sigma}^{l} \tag{5}$$

In which N^{*} is the modified nonlocal operator and is defined as follows [14]:

$$N^{*}=\sum_{i=0}^{\infty}\mu^{2i}L_e{}^{2i}\nabla^{2i} \tag{6}$$

It can be shown that the complete modified nonlocal Eq. (6) are a private solution of the nonlocal Eqs. (3). Omitting the middle-plane displacement of the plate, u_{p0} and v_{p0}, the nonlocal moment tensor and the nonlocal shear force tensor, respectively, are:

$$\mathbf{M}^{nl}=\begin{Bmatrix}M_x^{nl}\\M_y^{nl}\\M_{xy}^{nl}\end{Bmatrix}=\int_{-t_p/2}^{t_p/2}\begin{Bmatrix}\sigma_x^{nl}\\\sigma_y^{nl}\\\sigma_{xy}^{nl}\end{Bmatrix}z_p dz_p=-N^{*}\left(\frac{t_p^3}{12}\mathbf{C}\boldsymbol{\kappa}\right) \tag{7}$$

$$\mathbf{Q}^{nl}=\begin{Bmatrix}Q_x^{nl}\\Q_y^{nl}\end{Bmatrix}=\int_{-t_p/2}^{t_p/2}\begin{Bmatrix}\sigma_{xz}^{nl}\\\sigma_{yz}^{nl}\end{Bmatrix}dz_p=-N^{*}\left(D\begin{Bmatrix}\kappa_{x,x}+\kappa_{y,x}\\\kappa_{x,y}+\kappa_{y,y}\end{Bmatrix}\right) \tag{8}$$

In which:

$$D=\frac{E_p t_p^3}{12(1-\nu_p^3)} \tag{9}$$

The strain energy of the nanoplate can be written as follows:

$$U=\iiint\left(\sigma_x^{nl}\varepsilon_x+\sigma_y^{nl}\varepsilon_y+2\sigma_{xy}^{nl}\varepsilon_{xy}\right)dV=-\iint\left(M_x^{nl}\kappa_x+M_y^{nl}\kappa_y+2M_{xy}^{nl}\kappa_{xy}\right)dA \tag{10}$$

and if the plate is subjected to a distributed transverse load $q(x,y)$, the work done by the transverse load is:

$$W=\iint q(x,y)dA \tag{11}$$

The total potential energy of the nanoplate is obtained by $\Pi=U-W$, and applying the principle of virtual work, $\delta\Pi=0$, the governing equation of the nanoplate is obtained as follows:

$$N^*\left(D\nabla^4 w_p\right)=q \tag{12}$$

Also, making dimensionless relationships as following:

$$x=\frac{\pi x_p}{a_p},\ y=\frac{\pi y_p}{a_p},\ t=\frac{\pi t_p}{a_p}\ ,\ a=\pi,\ b=\frac{\pi b_p}{a_p},\ c=\frac{\pi c_p}{a_p},\ w=\frac{\pi w_p}{a_p} \tag{13}$$

and assuming isotropy and also constant thickness of the nanoplate, the governing differential equation of the nanoplates is obtained as follows:

$$N^*(\nabla^4 w)=\frac{qa_p^3}{\pi^3 D} \tag{14}$$

If the external length of the nanoplate be equal to its length, $L_e=a_p$, the modified nonlocal operator can be written as follows:

$$N^*=\sum_{i=0}^{\infty}\mu^{2i}\pi^{2i}\nabla^{*2i} \tag{15}$$

where in ∇^* was considered as the gradient in terms of dimensionless coordinate. Considering Levy's solution for the plate, shown in Fig. 1, the deflection equation of nanoplate with the dimensionless parameters is considered as follows:

$$w=w_1+w_2 \tag{16}$$

where in:

$$\begin{aligned} &w_1=\frac{4qa^3}{\pi^4 D}\sum_{n=1,3,\ldots}^{\infty}E_n n^{-5}\sin(nx)\quad ,\quad w_2=\sum_{n=1,3,\ldots}^{\infty}Y_n\sin(nx)\quad ,\\ &Y_n=\frac{qa^3}{D}[A_n\cosh(ny)+B_n ny\sinh(ny)+C_n\sinh(ny)+D_n ny\cosh(ny)] \end{aligned} \tag{17}$$

w_1 is the particular solution of the governing Eq. (14) and, w_2 is the general solution that their combination produces the overall solution equation. Placing w_1 in the equation of equilibrium (14), the following relationship is obtained:

$$\sum_{n=1,3,5,\ldots}^{\infty}E_n\left[\frac{\sin(nx)}{n}(1-n^2\mu^2\pi^2+n^4\mu^4\pi^4-n^6\mu^6\pi^6\pm\ldots)\right]=\frac{\pi}{4} \tag{18}$$

Due to the $\sum_{n=1,3,5,\ldots}^{\infty}\frac{\sin(nx)}{n}=\frac{\pi}{4}$, E_n can be achieved:

$$E_n=\frac{1}{\sum_{i=0}^{\infty}(-1)^i n^{2i}\mu^{2i}\pi^{2i}} \tag{19}$$

That for convergence E_n series and consequently, convergence of the Levy's solution should be either $\alpha = \mu^2\pi^2 n^2 < 1$ or $\mu < \frac{1}{n\pi}$. Also, based on the relationship (7), the dimensionless bending moment in the *x*-direction is defined as follows:

$$\overline{M}_y = \frac{a_p M_y}{\pi D} = -N^* \left(\frac{\partial^2 w}{\partial y^2} + \nu_p \frac{\partial^2 w}{\partial x^2} \right) \tag{20}$$

Following, the solution of the governing Eq. (14) is investigated in two cases. At first, Boundary conditions for all four edges are supposed simply-supported and then, for two transversal edges simply-supported (*x*=0) and two longitudinal edges clamped-supported (*y*=±*b*) are assumed.

2.1 Deflection of nanoplate in case of the Simply-Supported for all four edges

The nanoplate boundary conditions for this case are as follows:

$$\begin{aligned}
&(a)\ |y| \le b \ ,\ x = 0, \pi && w = 0 \ ,\ N^*\left(\frac{\partial^2 w}{\partial x^2}\right) = 0 \\
&(b)\ y = \pm b \ ,\ 0 \le x \le \pi && w = 0 \ ,\ N^*\left(\frac{\partial^2 w}{\partial y^2}\right) = 0 \\
&(c)\ y = 0 \ ,\ 0 \le x \le \pi && N^*\left(\frac{\partial^3 w}{\partial y^3} + (2-\nu_p)\frac{\partial^3 w}{\partial x^2 \partial y} \right) = 0 \\
&(d)\ y = 0 \ ,\ 0 \le x \le c \ ,\ \pi - c \le x \le \pi && \frac{\partial w}{\partial y} = 0 \\
&(e)\ y = 0 \ ,\ c \le x \le \pi - c && N^*\left(\frac{\partial^2 w}{\partial y^2} + \nu_p \frac{\partial^2 w}{\partial x^2} \right) = 0
\end{aligned} \tag{21}$$

In the above relationships, two relationships (a) and (b) represent four simply-supported for all four edges of the plate; relationship (c) indicates the zero shear force on the *x*-axis, due to the plate symmetry than the *x*-axis and also zero shear stress at the crack-free surface. relationship (d) with respect to symmetry than the *x*-axis, represents the zero deflection gradient in the section of the without crack of the plate along the *x*-axis, and the relationship (e) with respect to the zero normal stress in the crack-free surface, represents the zero bending moment in the crack-free surface. It should be noted that using the complete modified nonlocal theory, the nonlocal operator N^*, has appeared in the boundary conditions resulting from the obtained moment and shear force.

The boundary condition (a), from the set of boundary conditions (21), is established spontaneously in the governing Eq. (14) and can be obtained A_n, B_n by applying boundary conditions (b).

$$\begin{aligned}
A_n &= \frac{-4E_n}{\pi^4 n^5 \cosh(\beta)}\left[1 + \frac{\beta \tanh(\beta)}{2(1+\alpha)}\right] - C_n \tanh(\beta) - D_n\left[\frac{\beta}{\cosh^2(\beta)}\right] \ , \\
B_n &= \frac{2E_n}{(1+\alpha)\pi^4 n^5 \cosh(\beta)} - D_n \tanh(\beta)
\end{aligned} \tag{22}$$

In which $\beta = nb$. By applying boundary condition (c) from the set of boundary conditions (21), C_n obtain:

$$C_n = \left(\frac{1+\nu_p}{1-\nu_p} - 2\alpha\right) D_n \tag{23}$$

By placing C_n in relationships (22), the coefficients A_n, B_n in terms of D_n will obtain:

$$A_n = \frac{-4E_n}{\pi^4 n^5 \cosh(\beta)}\left[1+\frac{\beta\tanh(\beta)}{2(1+\alpha)}\right]-D_n\left[\frac{\beta}{\cosh^2(\beta)}+\left(\frac{1+\nu_p}{1-\nu_p}-2\alpha\right)\tanh(\beta)\right] \quad ,$$
$$B_n = \frac{2E_n}{(1+\alpha)\pi^4 n^5 \cosh(\beta)}-D_n\tanh(\beta) \tag{24}$$

Three coefficients A_n, B_n and C_n in terms of the coefficient D_n have been obtained and also, the coefficient D_n must be calculated from the other two boundary conditions.

By applying boundary condition (d) from the set of boundary conditions (21), the following relationship is obtained:

$$\sum_{n=1,3,\ldots}^{\infty}\left(\frac{2}{1-\nu_p}-2\alpha\right)nD_n\sin(nx)=0 \tag{25}$$

and finally, by applying boundary condition (e) from the set of boundary conditions (21) and after some algebraic operations, the following relationship is obtained.

$$\sum_{n=1,3,\ldots}^{\infty}(S_n-R_nD_n)\sin(nx)=0 \tag{26}$$

where in:

$$R_n = \frac{\beta n^2(1-\nu_p)}{(3+\nu_p)\cosh^2(\beta)}+n^2\tanh(\beta) \quad ,$$
$$S_n = -\frac{4\nu_p}{(3+\nu_p)\pi^4 n^3}-\frac{4E_n}{(3+\nu_p)\pi^4 n^3\cosh(\beta)}\left[1-\nu_p-\frac{1+(1-\nu_p)\alpha}{1+\alpha}+\frac{(1-\nu_p)\beta\tanh(\beta)}{2(1+\alpha)}\right] \tag{27}$$

Therefore the following equation-couple is obtained to achieve the coefficient D_n:

$$\sum_{n=1,3,\ldots}^{\infty} nP_nD_n\sin(nx)=0 \qquad 0\le x<c$$
$$\sum_{n=1,3,\ldots}^{\infty} R_nD_n\sin(nx)=\sum_{n=1,3,\ldots}^{\infty} S_n\sin(nx) \qquad c<x\le\frac{\pi}{2} \tag{28}$$

where in:

$$P_n = 1-\alpha(1-\nu_p) \tag{29}$$

If it is assumed that $R_nD_n = S_n + T_n$, the right side of the second Eq. (28) can be zeroed, then with determining T_n from the following two equations, D_n can be obtained.

$$\sum_{n=1,3,\ldots}^{\infty} n^{-1}(1+U_n)T_n\sin(nx)=P(x) \qquad 0\le x<c$$
$$\sum_{n=1,3,\ldots}^{\infty} T_n\sin(nx)=0 \qquad c<x\le\frac{\pi}{2} \tag{30}$$

where in:

$$P(x) = -\sum_{n=1,3,\ldots}^{\infty} n^{-1}(U_n + 1)S_n \sin(nx), \quad U_n = \frac{n^2 P_n}{R_n} - 1 \tag{31}$$

To determine T_n , It is assumed:

$$n^{-1}T_n = \int_0^c \varphi(t) J_0(nt) dt \tag{32}$$

and also using the following two equations [17]:

$$\begin{aligned} &2\sum_{n=1,3,\ldots}^{\infty} J_0(nt)\sin(nx) = H(x-t).(x^2-t^2)^{-\frac{1}{2}} + 2\int_0^{\infty}[1+\exp(\pi s)]^{-1} I_0(ts)\sinh(xs)ds \\ &2\sum_{n=1,3,\ldots}^{\infty} J_0(nt)\cos(nx) = H(t-x).(t^2-x^2)^{-\frac{1}{2}} \end{aligned} \tag{33}$$

In these two equations, the Heavyside Function is:

$$H(u) = \begin{cases} 0 & u < 0 \\ 1 & u > 0 \end{cases} \tag{34}$$

First, by placing T_n from the Eq. (32) in the second Eq. (30) and using the first Eq. (33), then, shift of the integral operator ordering and series, the result will obtain as following:

$$\int_0^c \varphi(t)[\sum_{n=1,3,\ldots}^{\infty} J_0(nt)\sin(nx)]dt = \int_0^c \varphi(t)[\frac{1}{2}H(x-t).(t^2-x^2)^{-\frac{1}{2}}]dt = 0 \tag{35}$$

Due to the $t - x < 0$, thus $H(x-t) = 0$, and as a result, the Eq. (35) becomes equal to zero and it satisfies the equation. By placing T_n from the Eq. (32) in the first Eq. (30), the following equation will obtain:

$$\sum_{n=1,3,\ldots}^{\infty} (1+U_n)[\int_0^c \varphi(t) J_0(nt)dt]\sin(nx) = P(x) \tag{36}$$

By placing the first Eq. (33) in the relationship (36), and after some algebraic operations and simplification, the state of Fredholm Integral Function of second kind is obtained:

$$\theta(\rho) + \int_0^1 \theta(r) K(\rho, r) dr = h(\rho) \tag{37}$$

where in $0 \le \rho \le 1$, and also:

$$\begin{aligned} &h(\rho) = -2\sum_{n=1,3,\ldots}^{\infty} (1+U_n) S_n J_0(n\rho c) \quad , \\ &\theta(\rho) = (\rho c)^{-1}\varphi(\rho c) \quad , \\ &K(\rho, r) = 2rc^2 \left\{ \int_0^{\infty} s[1+\exp(\pi s)]^{-1} I_0(rsc) I_0(\rho sc) ds + \sum_{n=1,3,\ldots}^{\infty} n U_n J_0(n\rho c) J_0(nrc) \right\} \end{aligned} \tag{38}$$

Thus, by numerical solution of the Fredholm Integral Function (37), which is given in the appendix, $\theta(\rho)$ will be obtained:

$$T_n = nc^2 \int_0^1 \rho\theta(\rho) J_0(n\rho c)d\rho \tag{39}$$

and consequently, D_n will be obtained:

$$D_n = \frac{S_n}{R_n} + \frac{nc^2}{R_n}\int_0^1 \rho\theta(\rho) J_0(n\rho c)d\rho \tag{40}$$

2.2 Deflection of nanoplate in the case: clamped-supported in y=± b and simply-supported in x=0, π

Boundary conditions of nanoplate, in this case, are as follows:

$$\begin{aligned}
&(a)\ |y| \le b \ ,\ x = 0,\pi && w = 0 \ ,\ N^*\left(\frac{\partial^2 w}{\partial x^2}\right) = 0\\
&(b)\ y = \pm b \ ,\ 0 \le x \le \pi && w = 0 \ ,\ N^*\left(\frac{\partial w}{\partial y}\right) = 0\\
&(c)\ y = 0 \ ,\ 0 \le x \le \pi && N^*\left(\frac{\partial^3 w}{\partial y^3} + (2-\nu_p)\frac{\partial^3 w}{\partial x^2 \partial y}\right) = 0\\
&(d)\ y = 0 \ ,\ 0 \le x \le c \ ,\ \pi - c \le x \le \pi && \frac{\partial w}{\partial y} = 0\\
&(e)\ y = 0 \ ,\ c \le x \le \pi - c && N^*\left(\frac{\partial^2 w}{\partial y^2} + \nu_p \frac{\partial^2 w}{\partial x^2}\right) = 0
\end{aligned} \tag{41}$$

All boundary conditions in this case are the same of the previous case, except the boundary condition (b). By applying boundary condition (b) to the set of boundary conditions (41), A_n and B_n will be obtained:

$$\begin{aligned}
A_n &= \frac{-4E_n}{\pi^4 n^5 \cosh(\beta)} - B_n \beta \tanh(\beta) - C_n \tanh(\beta) - D_n \beta \ ,\\
B_n &= \frac{4E_n \pi^{-4} n^{-5} \sinh(\beta) - C_n - D_n (1+2\alpha)\cosh^2(\beta)}{(1+2\alpha)\sinh(\beta)\cosh(\beta) + \beta}
\end{aligned} \tag{42}$$

The coefficient C_n is the same of the previous case. Therefore, by placing C_n from relationship (23) in the relationship (42), the coefficients A_n and B_n are simplified.

$$\begin{aligned}
A_n = {} & \frac{-4E_n}{\pi^4 n^5}\left[\frac{1}{\cosh(\beta)} + \frac{\beta\sinh(\beta)\tanh(\beta)}{(1+2\alpha)\sinh(\beta)\cosh(\beta)+\beta}\right]\\
& - D_n\left[\frac{-\left(\frac{1+\nu_p}{1-\nu_p}\right)\beta\tanh(\beta) - \beta\sinh(\beta)\cosh(\beta) - 2\alpha\beta\sinh^2(\beta)\tanh(\beta)}{(1+2\alpha)\sinh(\beta)\cosh(\beta)+\beta}\right]\\
& + \left(\frac{1+\nu_p}{1-\nu_p}\right)\tanh(\beta) - 2\alpha\tanh(\beta) + \beta \ ,
\end{aligned} \tag{43}$$

$$B_n = \frac{4E_n \sinh(\beta)}{\pi^4 n^5[(1+2\alpha)\sinh(\beta)\cosh(\beta)+\beta]} - D_n \left[\frac{\left(\frac{1+\nu_p}{1-\nu_p}\right) + \cosh^2(\beta) + 2\alpha\sinh^2(\beta)}{(1+2\alpha)\sinh(\beta)\cosh(\beta)+\beta} \right] \tag{43}$$

As in the previous case, the coefficients A_n, B_n and C_n have been obtained in terms of the coefficient D_n, Now, the coefficient D_n must be calculated from two other boundary conditions. Relationships (20) and (21) also satisfy this case. By replacing A_n and B_n from the relationship (43) in the relationship (25), the following equation obtains:

$$\sum_{n=1,3,\ldots}^{\infty} (\overline{S_n} - \overline{R_n} D_n)\sin(nx) = 0 \tag{44}$$

where in:

$$\begin{aligned} \overline{R_n} &= \frac{2\alpha n^2(3+\nu_p)(1-\nu_p)\sinh^2(\beta) - 4\alpha\beta n^2(1-\nu_p)^2\tanh(\beta) + 4\alpha(1-\nu_p)}{(3+\nu_p)((1+2\alpha)\sinh(\beta)\cosh(\beta)+\beta)} \\ &\quad + \frac{\beta^2 n^2(1-\nu_p)^2 - (1+\nu_p)^2\sinh^2(\beta) + 4\cosh^2(\beta)}{(3+\nu_p)((1+2\alpha)\sinh(\beta)\cosh(\beta)+\beta)} \quad , \\ \overline{S_n} &= -\frac{4\nu_p}{(3+\nu_p)\pi^4 n^3} - \frac{4E_n}{(3+\nu_p)\pi^4 n^3}\left[\frac{\beta(1-\nu_p)\cosh(\beta) - (1+\nu_p)\sinh(\beta)}{(1+2\alpha)\sinh(\beta)\cosh(\beta)+\beta} \right] \end{aligned} \tag{45}$$

As in the previous case, by solving two Eqs. (44) and (25), the state of the Fredholm Integral Function (second kind) is obtained:

$$\theta(\rho) + \int_0^1 \theta(r)\overline{K}(\rho, r)dr = \overline{h}(\rho) \tag{46}$$

where in:

$$\begin{aligned} &\overline{h}(\rho) = -2\sum_{n=1,3,\ldots}^{\infty} (1+\overline{U_n})\overline{S_n} J_0(n\rho c) \quad , \\ &\theta(\rho) = (\rho c)^{-1}\varphi(\rho c) \quad , \\ &\overline{K}(\rho, r) = 2rc^2\{\int_0^{\infty} s[1+\exp(\pi s)]^{-1} I_0(rsc) I_0(\rho sc)ds + \sum_{n=1,3,\ldots}^{\infty} n\overline{U_n} J_0(n\rho c) J_0(nrc)\} \\ &\overline{U_n} = \frac{n^2 P_n}{\overline{R_n}} - 1 \end{aligned} \tag{47}$$

and consequently, D_n will be obtained:

$$D_n = \frac{\overline{S_n}}{\overline{R_n}} + \frac{nc^2}{\overline{R_n}} \int_0^1 \rho\theta(\rho) J_0(n\rho c)d\rho \tag{48}$$

where in $\theta(\rho)$ is the solution of Fredholm Integral Function of the second kind (46), which must be calculated from numerical methods. Also, its solution is given in the Appendix.

2.3 Strain energy of a central cracked rectangular nanoplate under bending

Physically, strain energy values and stress intensity factor are important. Strain energy can be obtained by calculating the work done, and with applied load to the plate through its displacement:

$$U = \frac{1}{2}\int_A qw dA \tag{49}$$

This equation can be written as the sum of two relationships. The first relationship is the plate strain energy before the fracture and the second relationship is strain energy of the cracked plate which is limited to increase strain energy along the crack. Therefore, increase in strain energy resulting from the crack creation as follows:

$$\bar{U} = 2UD\pi^2 \Big/ q^2 a^6 = \int_{-b}^{b}\int_{0}^{\pi} [A_n \cosh(ny) + B_n ny \sinh(ny) + C_n \sinh(ny) + D_n ny \cosh(ny)]\sin(nx)dxdy \tag{50}$$

Because $D_n = 0$, corresponds to pre-fracture of the plate, terms that do not include D_n can be omitted and strain energy expansion determined by terms containing D_n. Therefore, for the central cracked nanoplate on the four simply-supported, the coefficients A_n and B_n, and C_n of the Eqs. (51) and the coefficient D_n of the Eq. (40) are calculated and placed in Eq. (50). According to this, the strain energy increase rate will be obtained:

$$\begin{aligned} A_n &= -D_n[\frac{\beta}{\cosh^2(\beta)} + (\frac{1+\upsilon}{1-\upsilon} - 2\alpha)\tanh(\beta)] \quad , \\ B_n &= -D_n \tanh(\beta) \quad , \\ C_n &= (\frac{1+\upsilon}{1-\upsilon} - 2\alpha)D_n \end{aligned} \tag{51}$$

For a central cracked nanoplate on two simply-support in x=0,π and two clamped-supported in y=±b, coefficients A_n, B_n and, C_n are calculated from the relationship (52) and also the coefficient D_n from the relationship (48). And then, they are placed in the relationship (50) to obtain the strain energy increase rate:

$$\begin{aligned} A_n &= -D_n[\frac{-(\frac{1+\upsilon}{1-\upsilon})\beta\tanh(\beta) - \beta\sinh(\beta)\cosh(\beta) - 2\alpha\beta\sinh^2(\beta)\tanh(\beta)}{(1+2\alpha)\sinh(\beta)\cosh(\beta) + \beta} \\ &\quad + (\frac{1+\upsilon}{1-\upsilon})\tanh(\beta) - 2\alpha\tanh(\beta) + \beta \quad , \\ B_n &= -D_n[\frac{\frac{1+\upsilon}{1-\upsilon} + \cosh^2(\beta) + 2\alpha\sinh^2(\beta)}{(1+2\alpha)\sinh(\beta)\cosh(\beta) + \beta}] \quad , \\ C_n &= (\frac{1+\upsilon}{1-\upsilon} - 2\alpha)D_n \end{aligned} \tag{52}$$

3 THE INVESTIGATION RESULTS AND ITS ANALYSIS

To validate the results obtained from the equations, in the equations of nonlocal elasticity theory can μ becomes equal to zero, until these equations transform into classical theory relationships. This comparison and validation were performed with reference [18]. As well as analysis using ABAQUS software to verify the obtained equations, was carried out. The non-cracked rectangular plate is assumed to have π-meter length, a variable width (0,2π] and

thickness 1mm, and also four simply-supported at its four edges. An elastic modulus 100 *GP*, a Poisson's ratio 0.25 and a distributed load 1 N/m^2, are considered. In the finite-element analysis, a square shell element with side length 5*cm* was used and its degrees of freedom in-plane (u=v=0) were constrained to be similar to Levy's solution. The comparison of strain energy is shown in Fig. 2, which shows very good conformity between the results. Also, in Levy's series, the numerical solution has been done for 200,000 sentences.

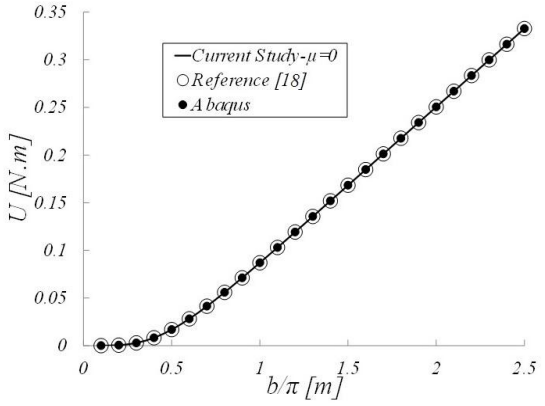

Fig.2
Strain energy of the non-cracked rectangular plate in terms of its width under distributed transverse load.

Then, the same of the previous plate was analyzed with a central crack all over the plate length. In the finite-element analysis, the nodes located on the crack were considered separately and the nodes were not merged to model the global longitudinal crack conditions. Then, for each plate width, strain energy resulting from the finite-element solution in the state of without crack (Fig. 2) was subtracted from strain energy obtained from the finite-element solution in the global longitudinal crack state. It was happened to obtain strain energy increase rate resulting from the crack creation and then, according to the relationship (50), became dimensionless. The comparison between the strain energy increase values caused by the creation crack in terms of the plate width is shown in Fig. 3, which shows very good conformity between the results.

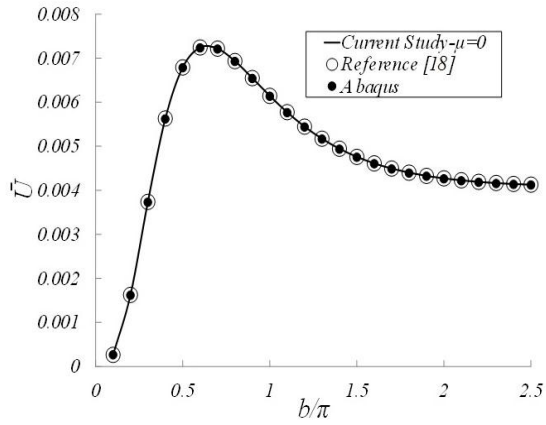

Fig.3
Strain energy of a rectangular plate with length π and a crack along its entire length, in terms of its width under distributed transverse load.

By comparing Figs. 2 and 3, it can be seen that total strain energy of the plate increases strongly with increasing plate width, but the strain energy increase value due to the global crack in the plate length, initially, increases with increasing plate width and then, in a specified width reaches a maximum value and converges to a specified number after some descent and never reaches zero. This indicates that the strain energy increase value of a plate with a large width, or an infinite width, and having a global central crack in the plate length, does not depend on the plate width and, it is a constant number dependent on the nanoplate length.

The percentage difference of the strain energy obtained from the complete nonlocal elasticity theory with reference [18] as well as with the ABAQUS results for the rectangular plate without crack and the global longitudinal crack under distributed transverse load in terms of its width are shown in Table 1.

Table 1
The percentage difference of the strain energy obtained from the results of the present study for 1. Non-cracked plate and also 2. Plate including a global longitudinal crack, in terms of its width with ABAQUS and reference [18].

	Without Crack		Completely Cracked	
b/π	Abaqus × 10^6 (%)	Reference [18] × 10^6 (%)	Abaqus × 10^6 (%)	Reference [18] × 10^6 (%)
0.1	0.121	0.027	1.095	0.118
0.2	0.597	-0.278	10.310	-0.140
0.3	0.913	-0.21	9.940	0.350
0.4	0.660	0.292	10.280	-0.370
0.5	0.249	0.105	8.804	0.049
0.6	0.348	-0.019	10.089	0.234
0.7	1.214	0.750	9.864	-0.294
0.8	2.864	-0.124	8.812	0.027
0.9	5.167	0.628	9.577	-0.072
1	8.146	0.656	10.000	0.425
1.1	11.442	0.843	10.001	-0.428
1.2	15.001	0.399	10.003	0.473
1.3	18.759	0.605	10.132	0.286
1.4	22.696	0.733	10.883	0.347
1.5	26.582	0.217	10.087	0.111
1.6	29.864	0.521	10.957	0.208
1.7	34.459	0.911	11.000	0.484
1.8	39.480	0.990	10.112	0.399
1.9	42.436	1.269	10.170	0.194
2	47.187	1.342	10.350	-0.110
2.1	51.188	1.420	10.101	0.224
2.2	55.750	1.058	9.181	0.426
2.3	58.869	1.009	11.387	-0.468
2.4	62.162	1.134	11.201	-0.239
2.5	67.306	1.355	9.010	-0.240

Additionally, the previous plate with a central crack was analyzed with a length less than the plate length, and also the plate width 0.4π was assumed. The diagram of the strain energy increase caused by the crack creation in terms of crack length was shown by Fig. 4.

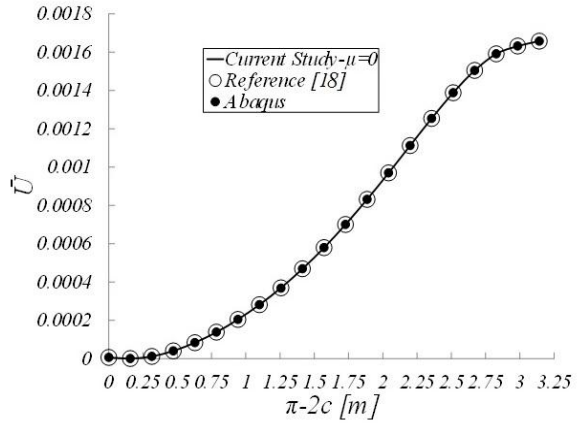

Fig.4
Strain energy of the central cracked rectangular plate with length π in terms of crack length for the plate width 0.4π.

As can be seen in Fig. 4, when the crack length is zero, the strain energy increase value caused by the crack creation is zero, and also with crack length increase, the strain energy increase value caused by crack creation, increased as is expected.

The percentage difference of the strain energy increase value obtained from the complete nonlocal elasticity theory with reference [18] as well as with the ABAQUS results for the rectangular plate with a central crack under distributed transverse load in terms of its length are shown in Table 2.

Table 2
The percentage difference of the strain energy increase value obtained from the results of the present study for the rectangular plate, with a central crack in terms of its length, with ABAQUS and reference [18].

$-2c/\pi$	Abaqus $\times$ 10^6 (%)	Reference [18] $\times$ 10^6 (%)
0	0.03%	0.08%
0.15708	0.03%	0.00%
0.314159	0.03%	0.00%
0.471239	0.21%	0.00%
0.628319	0.03%	0.00%
0.785398	0.0□%	0.00%
0.942478	0.03%	0.00%
1.099557	0.03%	0.00%
1.256637	2.01%	0.00%
1.413717	0.03%	-0.01%
1.570796	0.03%	0.00%
1.727876	0.03%	0.00%
1.884956	0.03%	0.00%
2.042035	0.03%	0.00%
2.199115	0.10%	0.00%
2.356194	0.02%	0.00%
2.513274	0.03%	0.00%
2.670354	0.03%	-0.01%
2.827433	0.03%	0.00%
2.984513	0.03%	0.00%
3.141593	0.21%	0.00%

As can be seen from Figs. 2 to 4, the results obtained from zeroing μ in the equations achieved from the modified nonlocal equations are consistent with reference [18] and the finite-element analysis, and also prove the accuracy of the relationships obtained.

After checking the validity of the equations with reference [18] and ABAQUS in the macro-scale, by placing the crack length equal to zero, the deflection of non-cracked nanoplate is obtained, that in this condition, the achieved results with reference [14], can be compared. Fig. 5 shows the ratio of the maximum deflection in terms of the small-scale effect for a non-cracked rectangular nanoplate that its length is twice its width and also, simply-supported were assumed at all of its edges. The results are compared with reference [14] and are shown there is good conformity between their results.

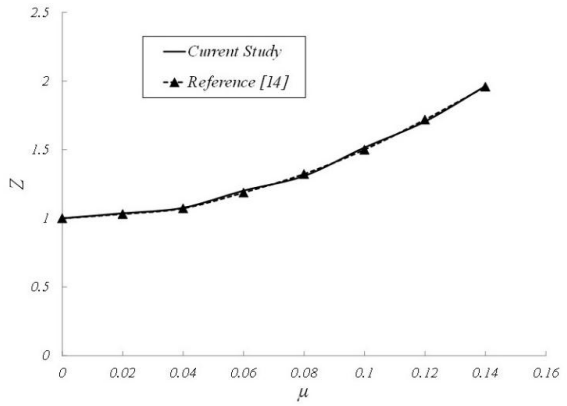

Fig.5
The ratio of the maximum deflection for a non-cracked rectangular nanoplate in terms of μ for four simply-supports at all of its edges.

In the calculations, the graphene nanoplate with the following properties are considered:

$$E_p = 903.37\ GPa \quad , \quad \nu_p = 0.25$$
$$L_i = 0.1396\ nm \quad , \quad L_e = 3.1974\ nm \quad , \quad b_p = 3.266\ nm \quad , \quad t_p = 0.335\ nm \tag{53}$$

In Fig. 6 was shown the deflection of the central cracked nanoplate, which has half of the plate length in y=0 in terms of x, for two simply-supported and clamped-supported. And in Figs. 7 and 8, the deflection of the same

nanoplate has drawn in the specified x in terms of y for the two states of simply-supported and clamped-support, respectively.

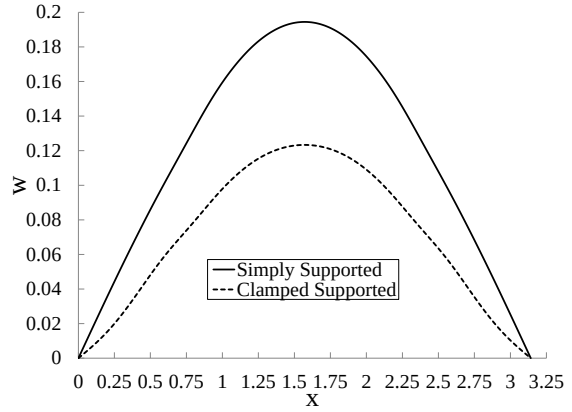

Fig.6
The deflection of the central cracked nanoplate in y=0 in terms of x for 1. Four simply-supported and 2. Two simply-supported in x=0,π and two clamped-supported in y=±b.

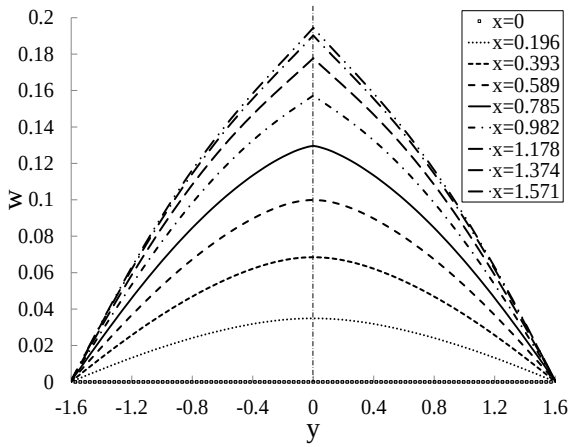

Fig.7
The deflection of the central cracked nanoplate under distributed transverse load on the four simply-supported in the specified x in terms of y.

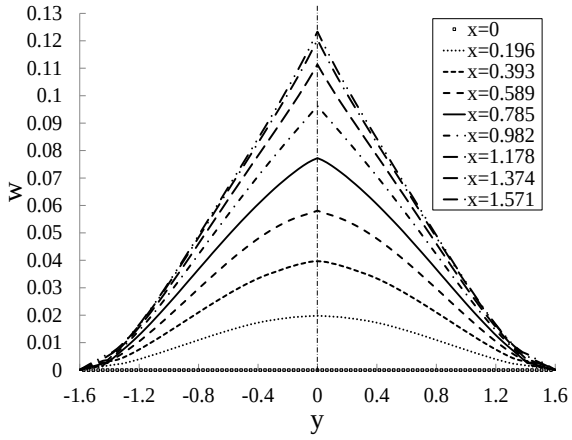

Fig.8
The deflection of the central cracked nanoplate under distributed transverse load on the two simply-supported in x=0,π and two clamped-supported in y=±b for the specified x in terms of y.

As can be seen in Fig.6, the deflection is higher on the four simply-supported than on the two simply-supported and clamped-supported, which is expected. Furthermore, according to Fig. 6, it is uniformly without fracture, but according to the two Figs. 7 and 8, the deflection in terms of y from the point x=0.785, where is the crack-tip, and after it, the crack line fracture, is obvious. The variations of the maximum deflection are shown in terms of μ for the central cracked nanoplate with half of the plate length for nanoplate on four simply-supported in Fig. 9. With the increase of μ, the maximum deflection has increased to the value that with reference [14] is consistent.

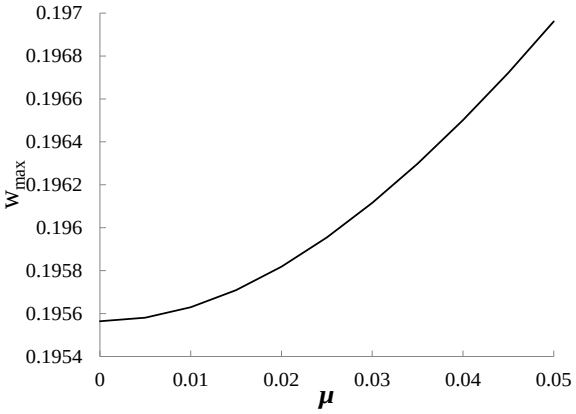

Fig.9
The diagram of the maximum deflection in terms of μ for the simply-supported.

Furthermore, the variations of the maximum deflection in terms of μ for the central cracked nanoplate with half of the plate length on two simply-supported and two clamped-supports is shown in Fig. 10. As can be seen, in this case, in contrast to the simply-supported, the maximum deflection has been increased with the increase of μ, and similar results have been acquired in reference [10].

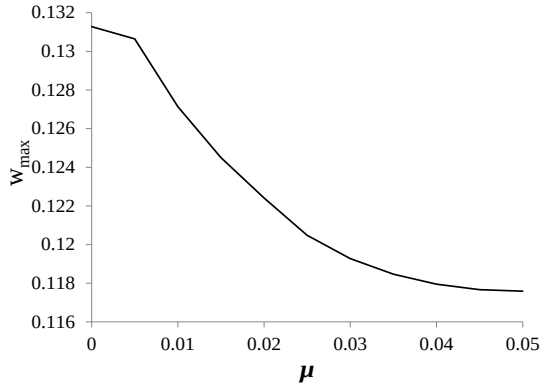

Fig.10
The maximum deflection in terms of μ for the state of on two simply-supported and two clamped-supports.

As stated, the condition for the deflection series convergence is $\mu<1/n\pi$. In order to see the effect "n" on the maximum deflection of the nanoplate for a specified value μ, the figure of the maximum deflection percentage difference was drawn according to Fig. 11. The percentage difference for n=27 was considered that its consequences $\mu<1/27\pi$. This figure was drawn for $e_0 = 0.25699$. As shown in Fig. 11, with rapid convergence, the error for n>11 is less than %1.

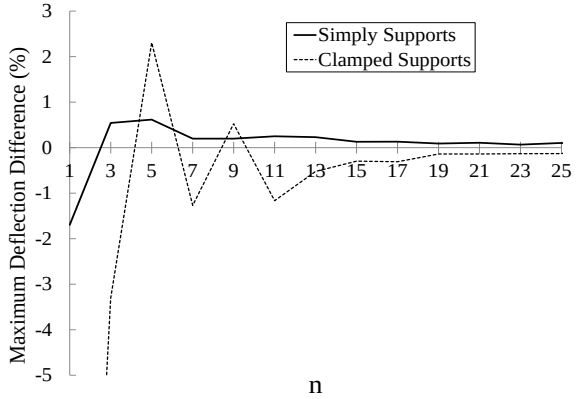

Fig.11
The maximum deflection percentage difference in terms of "n" for the nanoplate with $e_0 = 0.25699$.

In classical theory, there is a singularity at the crack-tip, and the value of stress or moment near the crack-tip does not indicate a defined value and tends to infinity. This lack is not observed in nonlocal elasticity theory, and

using this theory, a certain value of stress or moment can be obtained at the crack-tip. Also, there is not such singularity in the complete modified nonlocal elasticity theory. Fig. 12 shows the bending moment in terms of distance from the crack-tip for the previous nanoplate in the two state, including: two simply-supported and two clamped-supported. As can be seen, the bending moment has a definite value on the crack-tip (c-x=0) and there is not any singularity at the crack-tip, whereas the maximum bending moment is higher in the simply-supported state than in the clamped-supported state, as is expected.

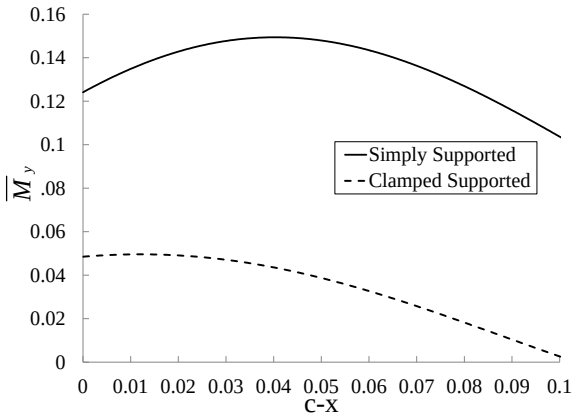

Fig.12
The moment diagram $\bar{M}_y$ in terms of c-x.

4 CONCLUSIONS

In this paper, using the complete modified nonlocal elasticity method, the strain energy and deflection equations of the rectangular nanoplate with a central crack under distributed transverse load in two states: four simply-supported at four edges, and two simply-supports at two edges and two clamped-supported at the other two edges, were obtained. To do this, by writing the governing equation for the nanoplate and using Levy's solution, it led to the solution of an equation-couple that must be solved simultaneously. By performing the mathematical operations and solving the mentioned equation-couple, a Fredholm Integral equation of second kind was obtained. The results of the present study show that:

- The convergence condition of solution is that it should always be $\mu \prec \frac{1}{n\pi}$.
- The strain energy increase value of the plate, with the global longitudinal crack along the plate length, and with a very large width does not depend on the plate width and is a constant value depending on the nanoplate length.
- In the clamped-supported state, the maximum deflection value increases slightly with increasing the value μ, but in the simply-supported state, the opposite happens.
- The convergence rate of deflection of the nanoplate is very high compared to the increase in the number of Levy's solution sentences, so that the error for n>11 is less than %1.
- Based on the nonlocal elasticity theory, there is not any singularity at the crack-tip.

APPENDIX

Solving Fredholm Integral equation (second kind) by the Mean Value Theorem (MVT).

The Fredholm Integral equation of second kind is assumed as follows:

$$\theta(\rho)+\int_0^1 \theta(r)K(\rho,r)dr = h(\rho) \tag{54}$$

with using the Mean Value Theorem can be written:

$$\theta(\rho) = h(\rho) - \theta(c').\int_0^1 K(\rho, r)dr \tag{55}$$

where c' is the average point length, which is between zero and one, and by placing $\rho = c'$ in the relationship (55), the following equation is obtained:

$$\theta(c') = \frac{h(c')}{1 + \int_0^1 K(c', r)dr} \tag{56}$$

Then, in the relationship (54) instead of $\theta(r)$ from the relationship (55) is placed:

$$\begin{aligned}\theta(\rho) &= h(\rho) - \int_0^1 \left[h(r) - \theta(c').\int_0^1 K(r, \eta)d\eta \right] K(\rho, r)dr \\ &= h(\rho) - \int_0^1 h(r)K(\rho, r)dr + \theta(c').\int_0^1\int_0^1 K(\rho, r)K(r, \eta)d\eta dr\end{aligned} \tag{57}$$

Then, again $\rho = c'$ is placed in the relationship (57).

$$\theta(c') = \frac{h(c') - \int_0^1 h(r)K(c', r)dr}{1 - \int_0^1\int_0^1 K(c', r)K(r, \eta)d\eta dr} \tag{58}$$

Now, the right side of the two relationships (56) and (58) be placed equal to each other.

$$\frac{h(c')}{1 + \int_0^1 K(c', r)dr} = \frac{h(c') - \int_0^1 h(r)K(c', r)dr}{1 - \int_0^1\int_0^1 K(c', r)K(r, \eta)d\eta dr} \tag{59}$$

As a result, c' from the following nonlinear equation solution is obtained using one of the numerical methods, for example, the Bisection Method.

$$h(c') = \frac{[\int_0^1 K(c', r)h(r)dr].[1 + \int_0^1 K(c', r)dr]}{\int_0^1 K(c', r)dr + \int_0^1\int_0^1 K(r, \eta)K(c', r)d\eta dr} \tag{60}$$

Eventually, by placing c' in the relationship (56), $\theta(c)$ is obtained and by placing it in the relationship (55), $\theta(\rho)$ is obtained.

List of English Symbols	
D	Bending module
e_0	The material intrinsic properties
E_p	Elastic module

J_0	Bessel's function of the zero-order
I_0	Modified Bessel's function of the zero-order
M	The Moment
N	The nonlocal operator
N^*	The modified nonlocal operator
L_e	The external length
L_i	The internal length
q	The Distributed transverse load
Q	The Shear force
t_p	The plate thickness
U	The total strain energy
$\bar{U}$	The strain energy increase value caused by the crack creation
u_p	The displacement in the direction x_p
v_p	The displacement in the direction y_p
w_p	The displacement in the direction z_p
Greek Symbols	
σ	Stress
ε	Strain
v_p	Poisson's ratio
μ	The small-scale effect parameter
k	Curvature
Subtitle	
p	Nanoplate
Superscript	
l	Local
nl	Nonlocal

REFERENCES

[1] Taheri A.H., 2009, *The Crack Study and Analysis on Nano-Dimensional Plates Based on the Expanded Finite Element Method*, K. N. Toosi University of Technology, Tehran, Iran.

[2] Gao J., 1999, An asymmetric theory of nonlocal elasticity – Part 2: Continuum field, *International Journal of Solids And Structures* **36**(20): 2959-297l.

[3] Zhou Z.G., Han J.C., Du S.Y., 1999, Investigation of a Griffith crack subject to anti-plane shear by using the nonlocal theory, *International Journal of Solids and Structures* **36**: 3891-3901.

[4] Zhou Z.G., Wang B., Du S.Y., 2003, Investigation of anti-plane shear behavior of two collinear permeable cracks in a piezoelectric material by using the nonlocal theory, *ASME Journal of Applied Mechanics* **69**: 388-390.

[5] Zhou Z.G., Shen Y.P., 1999, Investigation of the scattering of harmonic shear waves by two collinear cracks using the nonlocal theory, *Acta Mechanica* **135**: 169-179.

[6] Zhou Z.G., Wang B., 2003, Investigation of anti-plane shear behavior of two collinear impermeable cracks in the piezoelectric materials by using the nonlocal theory, *International Journal of Solids and Structures* **39**:1731-1742.

[7] Sun Y.G., Zhou Z.G., 2004, Stress field near the crack tip in nonlocal anisotropic elasticity, *European Journal of Mechanics A/Solids* **23**(2): 259-269,2004.

[8] Zhou Z.G., Wang B., 2003, Nonlocal theory solution of two collinear cracks in the functionally graded materials, *International Journal of Solids and Structures* **43**: 887-898.

[9] Huang L.Y., Han Q., Liang Y.J., 2012, Calibration of nonlocal scale effect parameter for bending single-layered graphene sheet under molecular dynamics, *NANO: Brief Reports and Reviews* **5**: 1250033-1250041.

[10] Yan J.W., Tong L.H., Li C., Zhu Y., Wang Z.W., 2015, Exact solutions of bending deflections for nano-beams and nano- plates based on nonlocal elasticity theory, *Composite Structures* **125**: 304-313.

[11] Rezatalab J., Golmakani M.E., 2015, Nonlinear bending analyzing of graphen nanoplate in polymeric environment using eringen nonlocal model, *22th Mechanical Engineering Conference,* Ahvaz, Iran.

[12] Şeref A., 2016, Static analysis of a nano plate by using generalized differential quadrature method, *International Journal of Engineering & Applied Sciences* **8**(2): 30-39.

[13] Eskandari Shahraki M., Heydari Bani M., Zamani M.R., Eskandari Jam J., 2018, Bending analyzing of graphen kirshoff nanoplate with simply supports using modified couple stress theory, *5th Mechanical Engineering Conference*, *Aerospace Industries*, Mashhad, Iran.

[14] Mousavi Z., Shahidi S.A., Boroomand B., 2017, A new method for bending and buckling analysis of rectangular nano plate: full modified nonlocal theory, *Springer* **52**(11): 2751-2768.

[15] Shvabyuk V., Pasternak I., Sulym H., 2011, Bending of orthotropic plate containing a crack parallel to the median plane, *Acta Mechanica et Automatica* **5**: 94-102.

[16] Chattopadhyay L., 2011, Analytical solution for bending stress intensity factor from reissner's plate theory, *Scientific Research Publishing* **3**: 517-524.

[17] Yang W.H., 1968, On an integral equation solution for a plate with internal support, *The Quarterly Journal of Mechanics and Applied Mathematics* **21**(4): 503-515.

[18] Keer L.M., Sve C., 1970, On the bending of cracked plates, *International Journal of Solids and Structures* **6**: 1545-1599.